ISSN 2616-7433 Vol. 2, Issue 11: 104-116, DOI: 10.25236/FSST.2020.021116

Analysis and Optimization of Aerodynamic Performance of Race Car Rear Wing Based on CFD

Kaicong Chen[1], Sen Liu[2]

1 Department of Applied Physics, Tongji University, Shanghai, 200092, China
2 Department of New Energy Science and Engineering, Xiamen University Malaysia, Kuala Lumpur, 43900 Sepang, Malaysia

ABSTRACT. *The most critical elements of the aerodynamic performance of a race car are the total downforce added on the wheels at high speed and the lift/drag ratio. This paper aims to analyze the aerodynamics of different shapes of a race car rear wing and give considerable optimization. Ansys-Fluent software will be used in this research, by adjusting the maximum cambers, maximum curvature positions and the angles of attack of a single rear wing, to find the best single-wing design, which gives the highest negative lift force and also lift/drag ratio. Then, the research will move forward to the effects of different wing slot sizes and aileron's angles of attack on the aerodynamics of multi-wing combinations.*

KEYWORDS: *Rear wing, Aerodynamic performance, CFD, Multi-wing combination*

1. Introduction

Aerodynamics is the key to success in motorsport. Aerodynamic designers have two primary concerns: First, creating downforce to bring the car's tyres closer to the track's ground, while improving the ability to turn; Second, reduce the air resistance caused by air turbulence to minimize the speed reduction. Since more than 2/3 of the grip of a race car is borne by the rear wheels, the negative lift force produced by rear wing has a significant impact on the dynamic performance and handling stability of race cars [1]. However, the existence of rear wing inevitably increases the aerodynamic drag of the race car. How to balance the downforce and aerodynamic drag has been a current concern of R & D engineers and related race car enterprises [2-3].

Lots of researches and experiments have been done to analyze the aerodynamic performance of race car rear wings. Yang Zhigang, et al [2] carried out numerical simulations to test the aerodynamics of different combinations of wings and found that increasing maximum camber and angle of attack helps to improve the lift coefficient of the rear wing. Coiro D P, et al [4] used both numerical and experimental methods, systematically studied the aerodynamic performance of a multi-element airfoil which was applied in rear wing. Kieffera W, et al [5] started an optimizing research of front wing on a Mazda Formula car, numerically computed the angle of attack and height from the ground, which showed the angle of attack had an impact on both lift and drag coefficient, while the height from ground influenced the lift coefficient.

This paper will analyze how different shapes, angles and combinations can affect the aerodynamic performance of inverted NACA 4-digit rear wings, and give reasonable optimization based on the computed results.

2. Main Procedures

2.1 Rear Wing Model Generation

Different negative lift wings will produce different aerodynamic effects. The race car rear wing is usually an inverted airfoil, which produces negative lift force due to the pressure difference caused by the different speeds of airflow across the upper and lower surfaces of the wing. However, race cars move at a slower speed compared with airplanes, according to formula (1):

$$Re = \frac{\rho V D}{\mu} \quad (1)$$

Where Re is the Reynolds number, ρ is the fluid density, V is velocity, D is the characteristic length of the

ISSN 2616-7433 Vol. 2, Issue 11: 104-116, DOI: 10.25236/FSST.2020.021116

object, μ is the viscosity of the fluid.

If the velocity is relatively low, the Reynolds number will decrease either, so race car rear wing cannot be simply generated by inverting the airfoil. In order to increase the lift force, the shapes of airfoil must be redesigned to give a higher lift force at low speed. The shape of the rear wing plays a major role in the aerodynamic performance. The airfoil's aerodynamic characteristics such as negative lift coefficient and lift/drag ratio are usually related to its angle of attack, the maximum camber and the maximum curvature position [8].

NACA 4-digit airfoil families were chosen in this research, the data set of certain airfoils can be generated based on formula 2 given below, where m is the maximum camber, p is the maximum curvature position, t is the maximum thickness and c is the chord length.

$$y_c = \frac{m}{p^2}(2px - x^2) \quad 0 \le x < p$$

$$y_c = \frac{m}{(1-p)^2}[(1-2p) + 2px - x^2] \quad p \le x \le c \tag{2}$$

$$\pm y_t = \frac{t}{0.2}(0.2969\sqrt{x} - 0.1260x - 0.3516x^2 + 0.2843x^3 - 0.1015x^4) \tag{3}$$

$$\begin{cases} x_U = x - y_t sin\theta \\ y_U = y_c + y_t cos\theta \end{cases}$$

$$\begin{cases} x_L = x + y_t sin\theta \\ y_L = y_c - y_t cos\theta \end{cases} \tag{4}$$

where $\theta = \arctan(\frac{dy_c}{dx})$

NACA Aerofoil Section Generator can be used to generate the 2D airfoil dataset, like Figure 1 shown below. The generated airfoil was NACA8516, where 8 means the 8%c maximum camber, 5 means 50%c maximum curvature position, 16 means 16%c maximum thickness and the default maximum thickness position is 30%c. The number of points was set to 81, which means 81 points in x-y plane will be generated to form an airfoil shape.

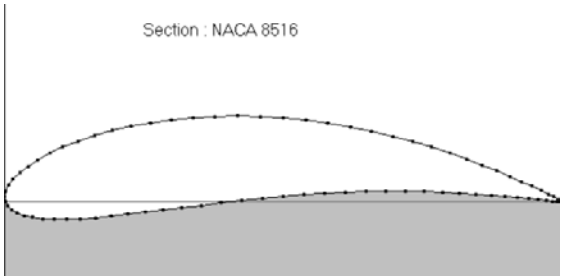

Fig.1 2d Naca8516 Airfoil Produced by Naca Aerofoil Section Generator

Once the dataset was generated, it was imported into AutoCAD, where the chord length, angle of attack, combination, and even the domain area of the rear wing can be defined.

(a) Single Rear Wing (b) Double-Wing Combination

Fig.2 (a) Adjusted Single Rear Wing and (B) Double-Wing Combination in Autocad

ISSN 2616-7433 Vol. 2, Issue 11: 104-116, DOI: 10.25236/FSST.2020.021116

2.2 Computation Domain

The computation domain chosen was a 2m x 4m rectangular area, the chord length of the rear wing was 0.3m, the position of rear wing's front edge vertex was (1m,1m). The left edge of the domain was velocity_inlet, the right edge was pressure_outlet, the side edges were defined to be no_slippery_wall.

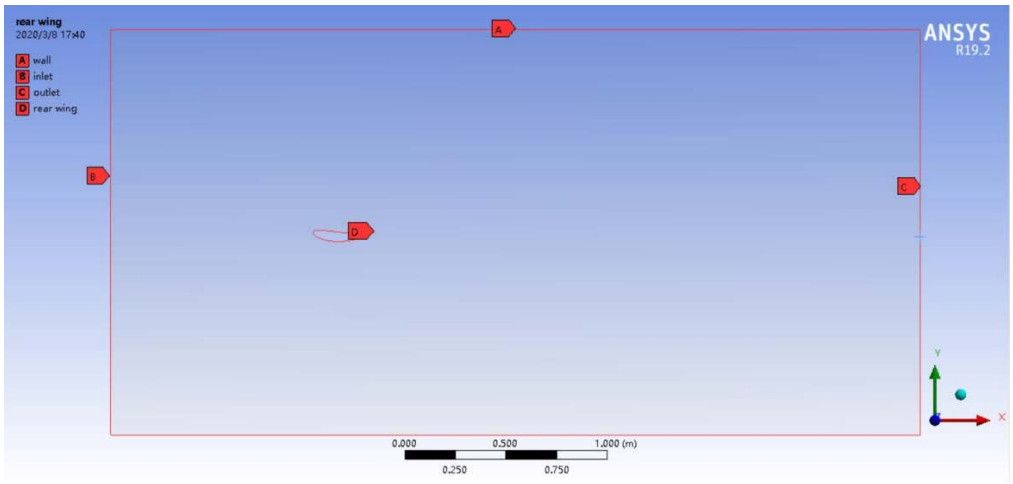

Fig.3 The Computation Domain

2.3 Mesh Optimization

In order to obtain more accurate results, mesh size optimization must be done before simulation[9]. While reducing the mesh element size step by step, the lift force, drag force of the NACA2516 rear wing and their ratio kept decreasing either. According to the observation, when the element size was reduced to 0.0075m (Domain) and 0.00075m (Rear Wing), the rate of value decreasing had been significantly reduced. Considering the calculation time and accuracy, 0.01m (Domain) and 0.001m (Rear Wing) was chosen to be the best mesh element size.

Table 1 Mesh Convergence Test

Domain (m)	Rear Wing (m)	Lift (N)	Drag (N)	L/D
0.1	0.01	-20.46	3.02	-6.78
0.05	0.005	-18.80	3.18	-5.91
0.03	0.003	-17.41	3.21	-5.42
0.02	0.002	-16.36	3.37	-4.85
0.01	0.001	-13.44	3.49	-3.85
0.0075	0.00075	-12.80	3.48	-3.68

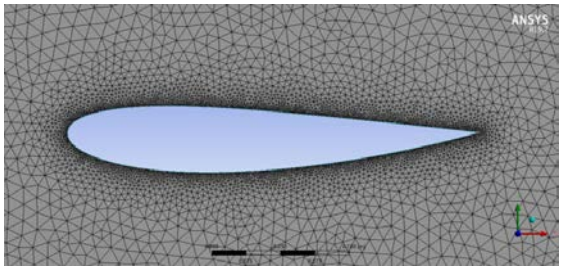

(a) NACA2516

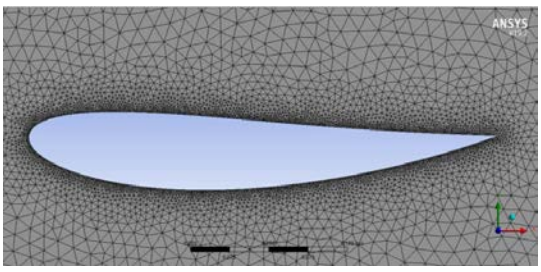

(b) NACA4516

ISSN 2616-7433 Vol. 2, Issue 11: 104-116, DOI: 10.25236/FSST.2020.021116

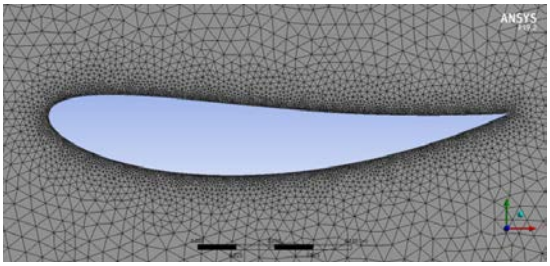
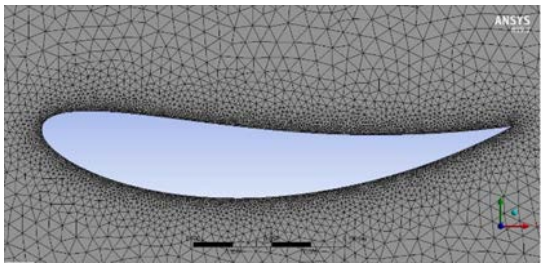

(c) NACA6516 (d) NACA8516

Fig.4 Rear Wing Grid of Final Plan

2.4 Turbulence Model

There are many viscous models in Fluent, such as laminar, K-epsilon et al., this paper will introduce k-epsilon turbulence model in detail.

K-epsilon is one of the turbulence model theories, K- ε model for short. The K- ε model is the most common turbulence model. It is based on the turbulent kinetic energy k and the turbulence dissipation rate ε, and it is a very prevalent two-equation model with reliability, good convergence and low memory demand. It has many sub-variants, such as Standard, RNG, Realizable, etc. [1]

a.Standard K- ε Model: The simplest complete turbulence model, it consists of two equations solving two variables (velocity and length). In Fluent, standard K- ε model has become the primary tool in engineering flow field simulation since it was proposed. It is economical, accurate and has a wide range of application. However, it's a semi-empirical formula, derived from experimental phenomena. For the standard k-epsilon model, its constant values are: k=1.0, σε=1.30, C1ε=1.44, C2ε=1.92,Cμ=0.09

For turbulent kinetic energy k [6]

$$\frac{\partial(\rho k)}{\partial t}+\frac{\partial(\rho k u_i)}{\partial x_i}=\frac{\partial}{\partial x_j}\left[\frac{\mu_t}{\sigma_k}\frac{\partial k}{\partial x_j}\right]+2\mu_t E_{ij}E_{ij}-\rho\varepsilon$$

For dissipation ε [6]

$$\frac{\partial(\rho\varepsilon)}{\partial t}+\frac{\partial(\rho\varepsilon u_i)}{\partial x_i}=\frac{\partial}{\partial x_j}\left[\frac{\mu_t}{\sigma_\varepsilon}\frac{\partial\varepsilon}{\partial x_j}\right]+C_{1\varepsilon}\frac{\varepsilon}{k}2\mu_t E_{ij}E_{ij}-C_{2\varepsilon}\rho\frac{\varepsilon^2}{k} \quad (5)$$

Where u_i represents velocity component in the corresponding direction

E_{ij} represents components of the rate of deformation

$$\mu=\rho C_\mu\frac{k^2}{\varepsilon}$$

b. RNG: RNG K- ε model is derived from strict technical statistics. It is similar to the standard K- ε model, but with the following improvements:

1) The Rng Model Adds a Condition to the Equation, Which Effectively Improves Accuracy;

2) Considering the Turbulent Vortex, the Accuracy in This Aspect is Improved.

3) Rng Theory Provides an Analytical Formula for the Turbulent Prandtl Number, Whereas the Standard K-E Model Uses User-Supplied Constants.

4) The Standard K- E Model is a High Reynolds Number Model. Rng Theory Provides an Analytical Formula for Flow Viscosity with Low Reynolds Number [1].

c. Realizable: Realizable K- ε model is different from the standard K- ε model in two major ways.

1) Realizable K- E Model Adds a Formula for Turbulent Viscosity: a New Transport Equation for the Dissipation Rate is Derived from an Exact Equation for Laminar Velocity Fluctuations.

2) The direct advantage of the Realizable K- ε model is that the divergence ratio of flat and cylindrical jets can be predicted more accurately, and it performs well in the analysis of rotating flow, boundary layer flow with

ISSN 2616-7433 Vol. 2, Issue 11: 104-116, DOI: 10.25236/FSST.2020.021116

a strong adverse pressure gradient, flow separation and secondary flow [1].

Due to the flow field around race car rear wing is generally steady, isothermal, incompressible, its complex shape will cause the separation of airflow, which should be treated as turbulence. In the following of this paper, Standard K- ε model would be used.

2.5 Parameter Setting

Table 2 Parameter Setting

Parameters	Setting
Viscous Model Fluid Fluid Density Fluid Viscosity	Standard k-epsilon Air 998.2kg/m^3 1.7894e-5 kg $m^{-1}s^{-1}$
Boundary Condition	Velocity-Inlet
	Pressure-Outlet
Velocity Magnitude	20m/s or 72kph
Turbulent Intensity	5%
Turbulent Viscosity Ratio	4739.45

2.6 Validation

In order to validate the accuracy of the simulation results, a 2D cylinder was simulated using the given settings at fixed Reynolds numbers. The 2D cylinder's diameter was 0.2m, the domain size (2m x 4m) and position(1m,1m) were the same as the rear wing.

Table 3 2D Cylinder Validation

Re	Condition	Velocity(m/s)	Drag(N)	Simulated Cd
40	Laminar	0.0029	2.2221E-06	2.1253
100	Laminar	0.0073	1.0118E-05	1.5484
10000	Turbulent-steady	0.7304	0.0714	1.0926
10000	Turbulent-transient	0.7304	0.0684	1.0469
100000	Turbulent-steady	7.3037	6.9323	1.0609
100000	Turbulent-transient	7.3037	6.9060	1.0568

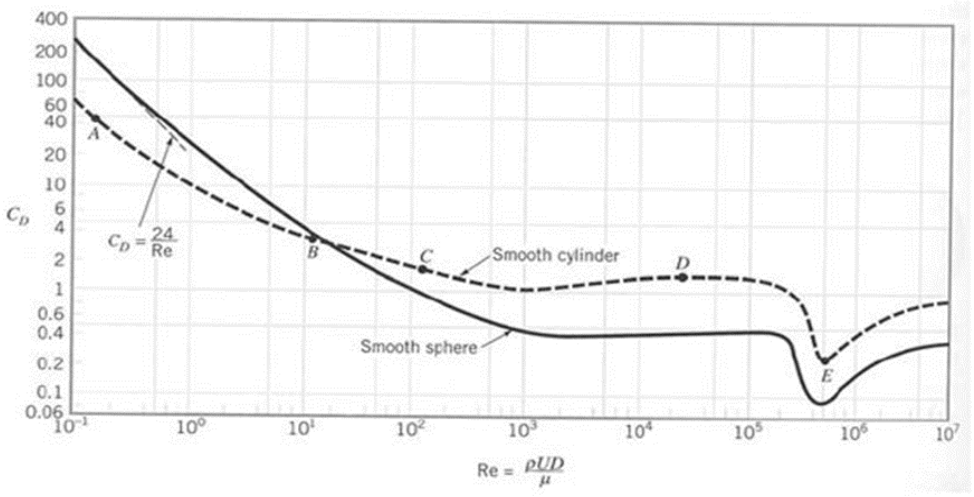

Fig.5- the Theoretical Cd-Re Plot of Circular Cylinder [7]

ISSN 2616-7433 Vol. 2, Issue 11: 104-116, DOI: 10.25236/FSST.2020.021116

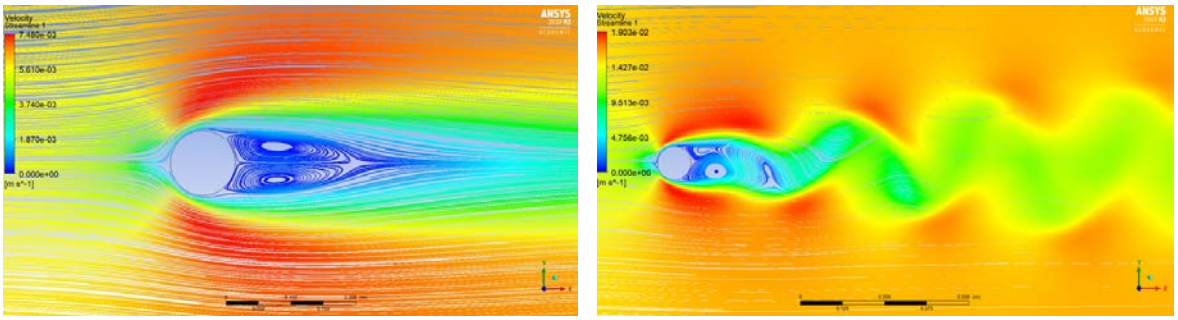

(a) Streamline Field at Re=40 (b) Streamline Field at Re=100

Fig.6 Streamline Field of 2d Cylinder At (a) Re=40 and (B) Re=100

According to Figure 5, it was clear that the simulated results were reasonable and accurate compared with theoretical ones. Meanwhile, the turbulent-steady results were roughly the same as the turbulent-transient results, considering both calculation time and accuracy, turbulent-steady model would be used in this paper.

Figure 6 showed the streamlines of air at certain Reynolds numbers, when the Reynolds number was equal to 40, symmetrical vortexes appeared behind the cylinder, when Re was 100, Karman vortex appeared as predicted. These phenomena further verified the accuracy of the validation.

3. Results & Analysis

3.1 Single Rear Wing

Table 4 Aerodynamic Performance of Different Max Camber

(a) Max Camber 2% (Inverted NACA2516) (b) Max Camber 4% (Inverted NACA4516)

Angle of Attack(°)	Lift (N)	Drag (N)	L/D Ratio		Angle of Attack(°)	Lift (N)	Drag (N)	L/D Ratio
0	-13.4410	3.4923	-3.8488		0	-23.5020	3.7065	-6.3408
5	-45.6580	4.6505	-9.8179		5	-60.3790	5.1038	-11.8302
10	-73.4910	8.0781	-9.0976		10	-87.3790	8.5099	-10.2679
15	-90.7310	13.1720	-6.8882		15	-103.1300	13.8970	-7.4210
20	-87.4240	20.0580	-4.3586		20	-102.3000	20.5280	-4.9834
25	-82.6310	28.2740	-2.9225		25	-91.0220	29.5650	-3.0787

(c) Max Camber 6% (Inverted NACA6516) (d) Max Camber 8% (Inverted NACA8516)

Angle of Attack(°)	Lift (N)	Drag (N)	L/D Ratio		Angle of Attack(°)	Lift (N)	Drag (N)	L/D Ratio
0	-41.5116	4.0885	-10.1533		0	-53.5748	4.6829	-11.4405
5	-73.5709	5.6720	-12.9708		5	-85.4681	6.4041	-13.3458
10	-100.9884	9.1927	-10.9858		10	-110.7759	9.8073	-11.2952
15	-115.6957	14.4089	-8.0295		15	-126.0313	14.9792	-8.4138
20	-114.8135	21.2801	-5.3953		20	-125.4299	21.6840	-5.7845
25	-107.0193	30.0786	-3.5580		25	-116.4460	30.4258	-3.8272

ISSN 2616-7433 Vol. 2, Issue 11: 104-116, DOI: 10.25236/FSST.2020.021116

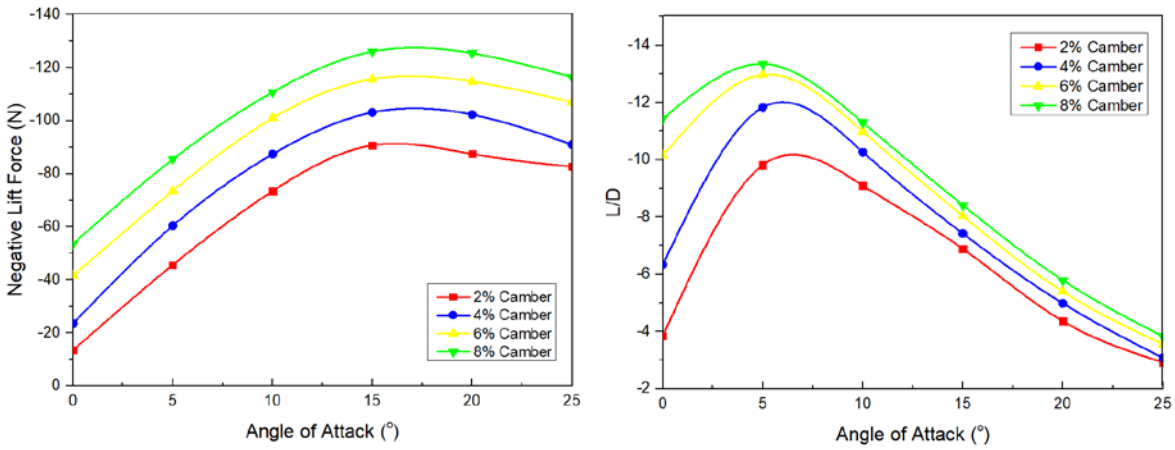

(a)Lift VS. Angle of Attack Plot (b) L/D Ratio VS. Angle of Attack Plot

Fig.7 - (a) Lift VS. Angle of Attack Plot and (B) l/d Ratio VS. Angle of Attack Plot

According to Figure 7(a), as the maximum camber of rear wing increases, the maximum negative lift force of rear wing increases too. So, increasing the rear wing's maximum camber within limits is considered to be one of the most effective methods to increase the maximum negative lift force.

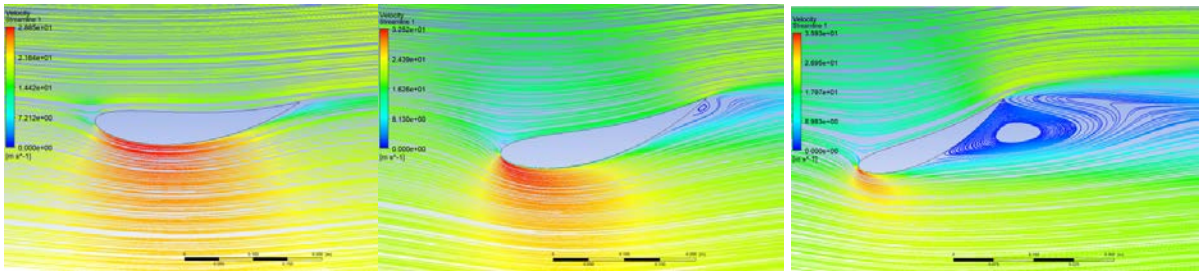

(a)5° (b) 15° (c) 25°

Fig.8 - Streamline Field Around Rear Wing At Certain Angle of Attack

However, the angles of stall of different rear wings are not much difference according to Figure 7(a) (around 15°). The reason for stall can be clearly seen in Figure 8. When the angle of attack increases to a certain degree, the separation of the airflow at the tail of the wing will result in vortexes, which will affect the lift force dramatically.

Lift/drag ratio refers to the ratio of negative lift force to the drag force produced by rear wing. With the increase of maximum camber of the rear wing, its lift/drag ratio increases too, and the lift/drag ratio of any rear wing with the larger camber is higher than that of the rear wing with the relatively smaller maximum camber. At a relatively small angle of attack, the lift/drag ratio of each rear wing varies greatly. However, with the increase of the angle of attack, the difference of lift/drag ratio of each rear wing decreases gradually. At 25°, the lift/drag ratio of all rear wings are all around 3~4.

Comparing the aerodynamic performance of all the rear wings, the rear wing with 8% maximum camber was considered to be the best design. Therefore, it would be chosen to be the main wing in the following double-wing system analysis.

ISSN 2616-7433 Vol. 2, Issue 11: 104-116, DOI: 10.25236/FSST.2020.021116

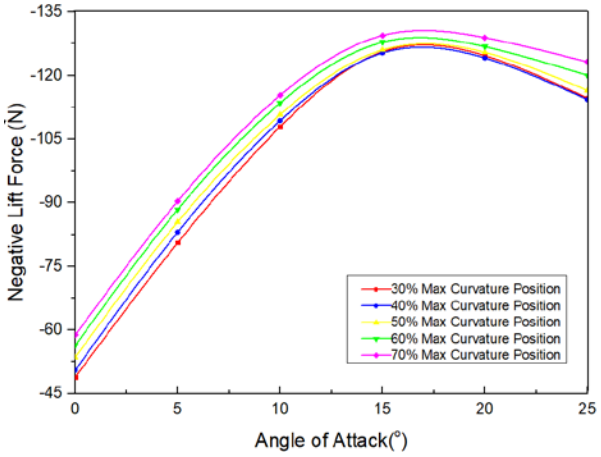

Fig.9 Negative Lift Force of Rear Wings with Different Max Curvature Position

The maximum curvature position of the wing is expressed as a percentage of the chord length. Changing the maximum curvature position of the wing will change the pressure distribution on the wing surface, thus optimizing negative lift force and stall rate [8]. In this step, the maximum curvature position of NACA8516 rear wing would be changed to 30%, 40%, 60%, 70% of the chord length and then put into CFD analysis. The trend of the change of negative lift forces of rear wings is given in Figure 9. With the increase of the maximum curvature position, the negative lift force also increases gradually. Although the stall angle doesn't change much, the stall rate decreases slightly.

3.2 Double-Wing Combination

3.2.1 Principle

From the previous section, the primary way to obtain more negative lift force with a single fixed-shape rear wing, is to increase the angle of attack. But when the angle of attack is increased to a certain level, vortexes will be produced, which can create a tremendous drag on a fast racing car and affect its aerodynamic performance significantly. In order to obtain a large, stable, reliable and even adjustable negative lift force, the double-wing combination will be analyzed.

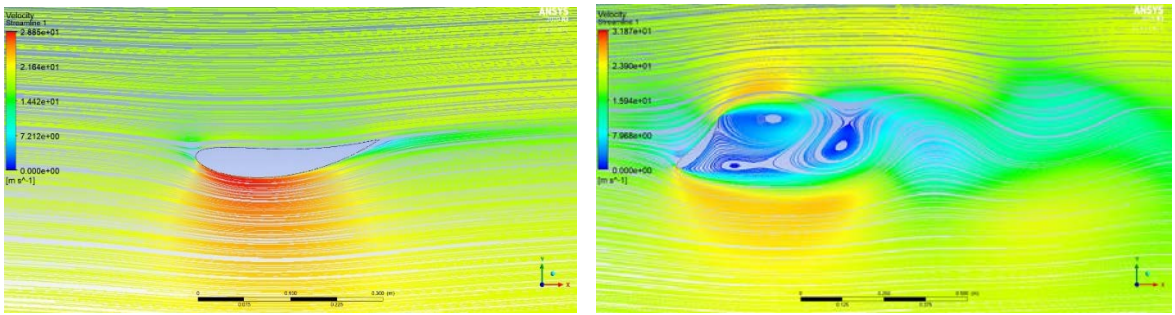

(a) Main Wing, 5 Degree Angle of Attack (b) Aileron, 50 Degree Angle of Attack

Fig.10 (a) Inverted Naca8516 Main Wing, 5 Degree Angle of Attack. 0.3m Chord Length and (b) Inverted NACA8516 Aileron, 50 Degree Angle of Attack. 0.2m Chord Length

Table 5 Aerodynamic Performance of Double-Wing Combination

5° Main Wing Alone	-85.47	6.40	-13.3458
50° Aileron Alone	-63.11	64.91	-0.9724
Numerical Sum	-148.58	71.31	-2.0836
2-Wing Combination	-315.16	58.54	-5.3839

ISSN 2616-7433 Vol. 2, Issue 11: 104-116, DOI: 10.25236/FSST.2020.021116

The numerical sum of the negative lift force and drag force of main wing and aileron shown in Figure 10 are -148.58N and 71.31N respectively. However, when putting two wings together, like Figure 11 (a), the negative lift force produced soared to 315.16N and drag force decreased to 58.54N, the vortexes also disappeared completely. The reason for this is that the aileron rectifies the airflow behind the main wing, eliminating vortexes while maintaining a large angle of attack of 50 degrees, thus increases negative lift significantly.

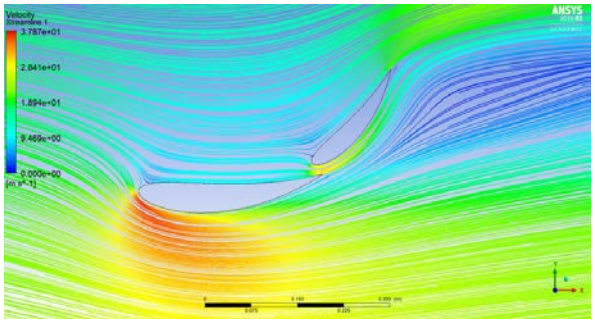

(a) 18mm Left to The Main Wing

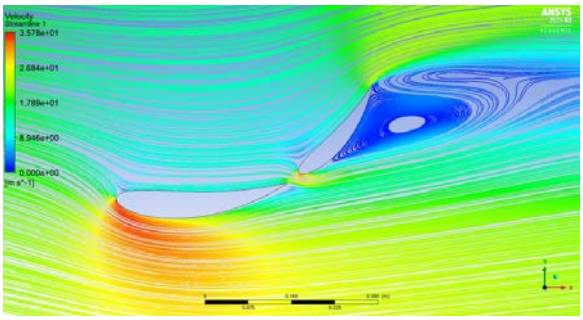

(b) 18mm Right to The Main Wing

Fig.11 (a) Aileron is 18 Mm Above,18mm Left to the Main Wing (B) Aileron is 18 Mm Above,18mm Right to the Main Wing

The most critical parameter of the double-wing combination is the slot size between the trailing-edge of the main wing and the leading-edge of the aileron. When the air flows through the upper surface of the main wing and finally reaches the trailing-edge, it will be accelerated by the narrow slot, becomes much faster than the air flowing through the lower surface of the main wing. The function of this narrow slot is to control the boundary layer of the wing and delay airflow separation, so that even if the aileron's angle of attack is very large, the high-energy airflow still can adhere to it, thus prevents the generation of vortexes. Compared with the single-wing, the double-wing combination has relatively larger curvature, which significantly delays the stall angle and generates more negative lift force [8].

The aileron's leading-edge is suggested to be placed on the inner side of the main wing's trailing-edge. This is because when the aileron's leading-edge is placed on the right side, like Figure 11 (b), only a small amount of airflow will run to the lower surface of the aileron through the slot. Since there is not enough airflow passing through the wing slot, it is impossible to control the boundary layer of the aileron and delay the airflow separation. In this case, the turbulence produced will result in extremely high drag force on a high-speed race car.

3.2.2 Model Generation

The main wing and aileron are usually in the same shape, and the chord length of the aileron is usually 30% - 40% of the chord length of the whole wing combination. (The distance from the leading-edge of the main wing to the trailing-edge of the last aileron) [10-11]

In this paper, the chord length of main wing and aileron were 0.3m and 0.2m respectively. The angle of attack of the main wing was 5 ° (The maximum lift/drag ratio design). The aileron's angles of attack were set to 40°, 45° and 50°. The size of mesh and computation domain were the same as the previous section.

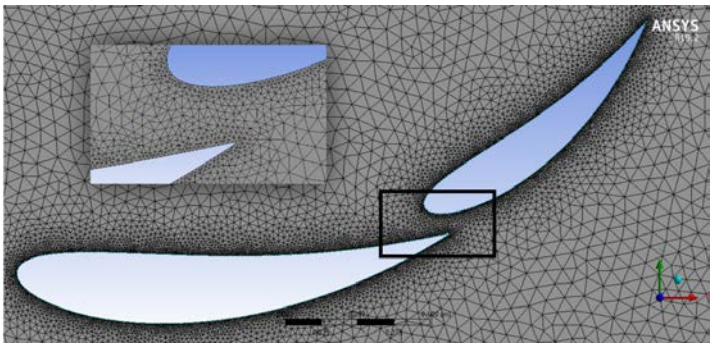

Fig.12 The Mesh of Double-Wing Combination (X=18, y=18, Aileron 40°)

ISSN 2616-7433 Vol. 2, Issue 11: 104-116, DOI: 10.25236/FSST.2020.021116

The slot size was divided into the horizontal distance (the horizontal distance between the leading-edge of the aileron and trailing-edge of the main wing) and the vertical distance (the vertical distance between the leading-edge of the aileron and trailing-edge of the main wing). The horizontal distance and vertical distance were ranging from 2% (6mm) to 6% (18mm) of the main wing's chord length. The following of this paper will analyze the influence of slot size and aileron's angles of attack on the aerodynamic performance of the double-wing combination.

3.2.3 Simulation Results

Table 6 Aerodynamic Performance of Different Slots of Double-Wing Design with 40^o Aileron

Horizontal Distance (mm)	Vertical Distance (mm)	Lift(N)	Drag(N)	L/DRatio
6	6	-286.20	40.08	-7.1413
6	9	-296.57	42.16	-7.0349
6	12	-303.79	43.53	-6.9795
6	15	-308.02	44.73	-6.8859
6	18	-313.63	45.11	-6.9530
9	6	-281.67	40.36	-6.9796
9	9	-295.27	42.24	-6.9910
9	12	-302.07	43.71	-6.9113
9	15	-307.20	44.40	-6.9186
9	18	-312.63	45.35	-6.8931
12	6	-280.59	40.19	-6.9814
12	9	-291.63	42.38	-6.8816
12	12	-301.06	43.83	-6.8687
12	15	-304.90	44.85	-6.7976
12	18	-310.51	45.30	-6.8544
15	6	-279.90	40.33	-6.9406
15	9	-290.42	42.46	-6.8399
15	12	-300.00	43.76	-6.8551
15	15	-303.46	44.93	-6.7548
15	18	-308.25	45.59	-6.7611
18	6	-279.80	40.72	-6.8715
18	9	-289.86	42.50	-6.8196
18	12	-297.85	43.79	-6.8026
18	15	-303.01	44.69	-6.7809
18	18	-306.34	45.46	-6.7393

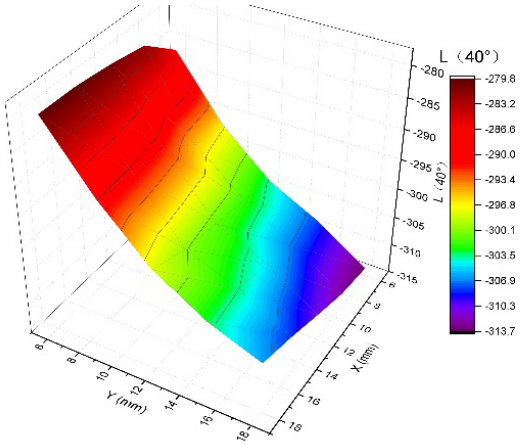

(a) 40° Aileron

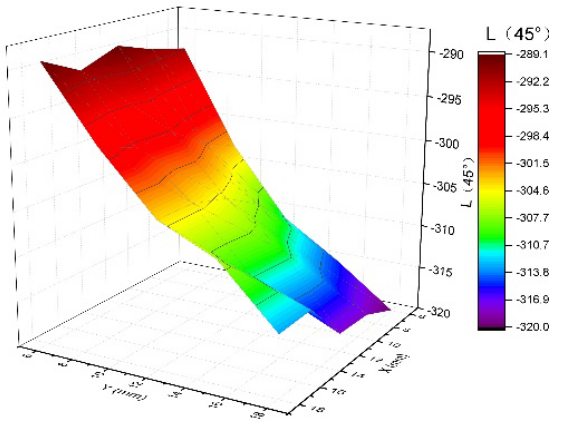

(b) 45° Aileron

ISSN 2616-7433 Vol. 2, Issue 11: 104-116, DOI: 10.25236/FSST.2020.021116

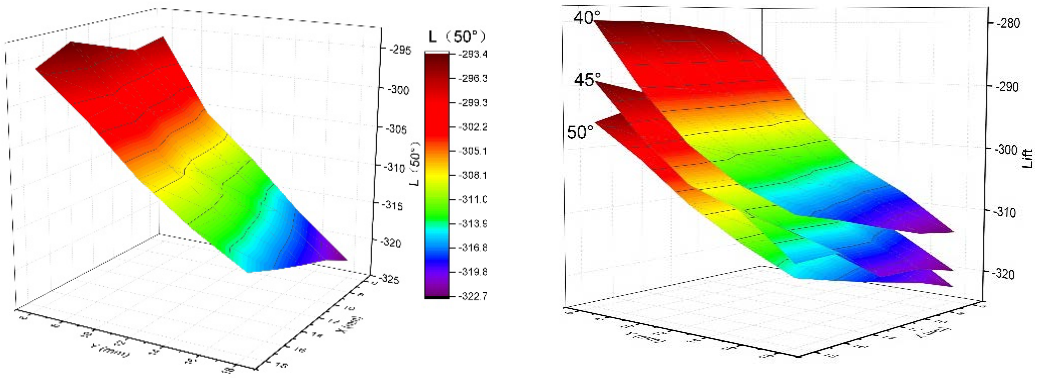

(c) 50° Aileron (d) Comparison

Fig.13 the Negative Lift Force of Each Double-Wing Combination

The influence of horizontal distance(X), vertical distance(Y) and aileron angle of attack on negative lift force are shown in figure 13. The trend of lift variation can be summarized as:

1) Negative Lift Force Increases Almost Linearly with the Increase of Vertical Distance(y).

2) The Change of Horizontal Distance(X) Has a Very Limited Effect on Negative Lift Force.

3) The aileron's Angle of Attack Has a Clear Influence on the Negative Lift Force. According to the Comparison, Aileron with 50° Angle of Attack Produced the Largest Negative Lift Force.

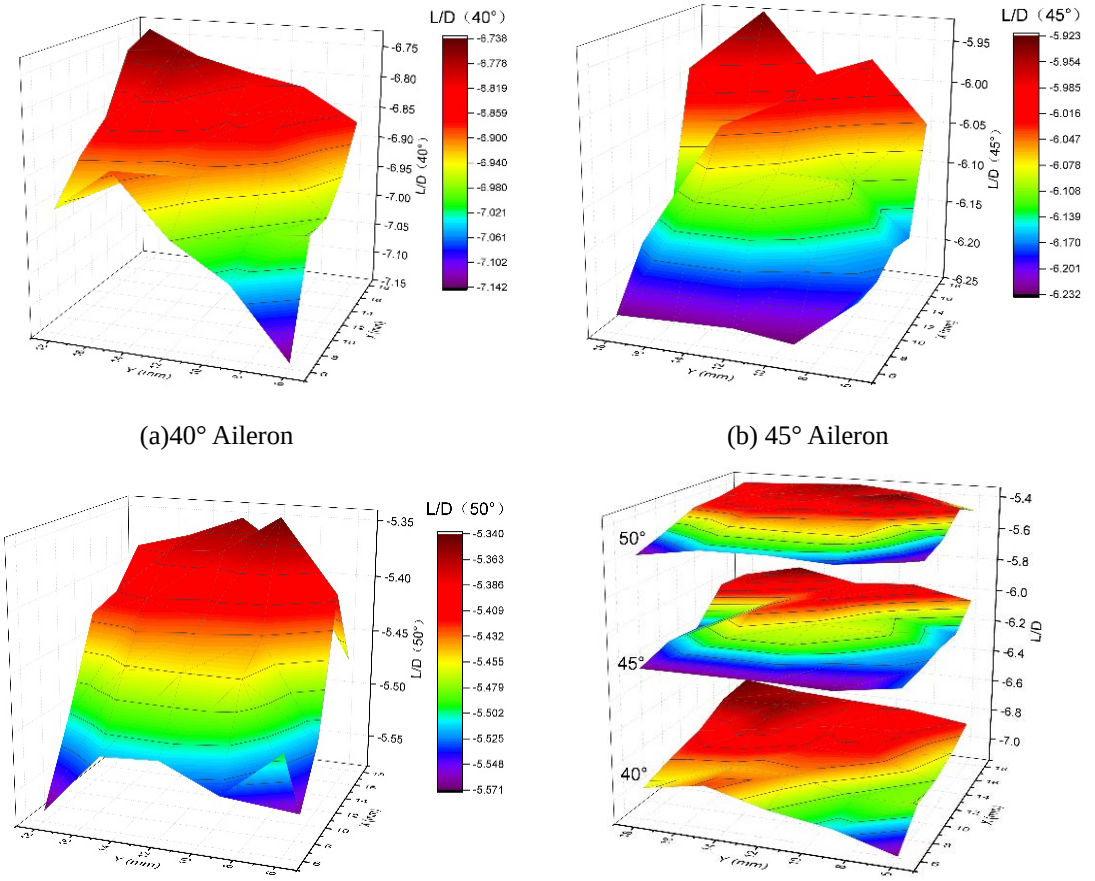

(a)40° Aileron (b) 45° Aileron

(c) 50° Aileron (d) Comparison

Fig.14 the Lift/Drag Ratio of Each Double-Wing Combination

ISSN 2616-7433 Vol. 2, Issue 11: 104-116, DOI: 10.25236/FSST.2020.021116

The influence of horizontal distance(X), vertical distance(Y) and aileron angle of attack on lift/drag ratio is shown in figure 14. The trend of lift/drag ratio variation can be summarized as:

1) When the aileron's Angle of Attack is 40°, the Lift/Drag Ratio Decreases with the Increase of X and y, and the Effects of Both X and y on the Lift Drag Ratio Are Similar

2) For Aileron At 45 ° (Fig. B) and 50 ° (Fig. C), the Lift/Drag Ratio Decreases Mainly with the Increase of X, the Effect of y is Not as Great as X.

3) The Aileron Angle Has a Relatively Larger Influence on the Lift/Drag Ratio When the Aileron is 40°.

3.3 Multi-Wing Combination

Table 7 Aerodynamic Performance of Multi-Wing Combination

Combination	Lift (N)	Drag (N)	L/D Ratio
3-Wing	-373.90	69.60	-5.3724
4-Wing	-402.95	82.17	-4.9038

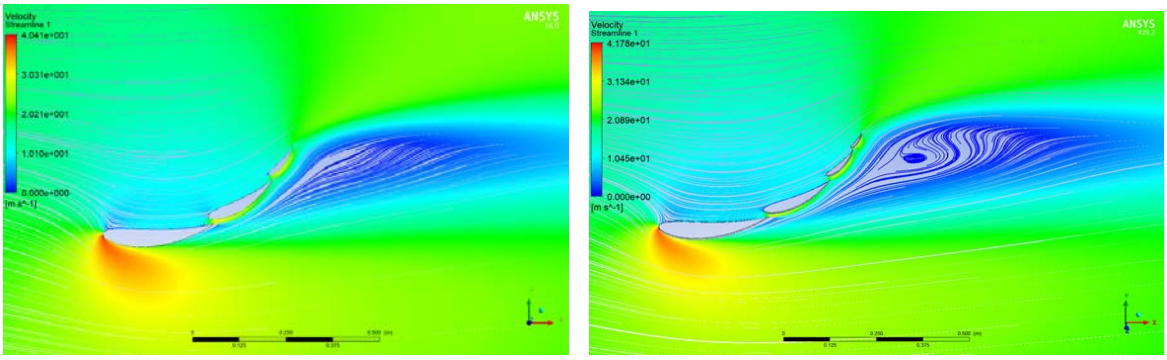

(a) 3-Wing Combination (b) 4-Wing Combination

Fig.15 Streamline Field of Different Multi-Wing Combinations

From Figure 15, It can be seen that the negative lift force generated by the 3-wing combination was not much lower than that of the 4-wing combination. However, the turbulence was effectively avoided in 3-wing combination and the lift/drag ratio was also higher.

In general, the 3-wing combination would be a better choice in terms of low drag force, high lift/drag ratio and good stability.

4. Conclusion

In this paper, the influence of aerodynamic parameters (angle of attack, maximum camber, maximum curvature position, wing slot size) on the aerodynamic performance of a single race car rear wing and a multi-wing combination were analyzed. The main results are summarized as:

1) With the Increase of Maximum Camber of the Rear Wing, the Negative Lift Force and Lift/Drag Ratio Increase.

2) For an Inverted Naca8516 Rear Wing, the Highest l/d Ratio Appears When the Angle of Attack is 5^o, the Stall Angle is Around 15^o, the Maximum Negative Force Appears When the Angle of Attack is 15^o.

3) With the Increase of the Maximum Curvature Position, the Negative Lift Force Increases, the Stall Rate Decreases.

4) The Existence of Aileron Can Efficiently Increase Negative Lift Force and Avoid Turbulence.

5) The Size of the Wing Slot and aileron's Angle of Attack Are the Key to the Design of the Multi-Wing Combination.

ISSN 2616-7433 Vol. 2, Issue 11: 104-116, DOI: 10.25236/FSST.2020.021116

6) Multi-Wing Combination Can Generate More Negative Lift Force, But Assembling Too Many Wings Will Enhance the Drag Force and Reduce the l/d Ratio.

References

[1] Zhu Shizhuo, Wang Yu, Cheng Shi, et al (2019). Simulation Analysis and Development of Aerodynamic Structure of Formula One Racing Car. Automobile Times.
[2] Yang Zhigang, Gu Wenjun, Li Qiliang (2011). Aerodynamic Design Optimization of Race Car Rear Wing. Ieee International Conference on Computer Science and Automation Engineering.
[3] Mao Xu, Wu Ningning (2014). Aerodynamic Performance Improvement of a New Type Wing for Formula Sae Car. Mechanical Science and Technology for Aerospace Engineering, vol.v3, no.9, pp.1397-1402.
[4] Coiro D P, Nicolosi F, Amendola A, Barbagallo B, et al (1997). Experiments and Numerical Investigation on A Multi-Component Airfoil Employed in A Racing Car Wing [J]. SAE Special Publications, pp. 221-226.
[5] Kieffera W, Moujaesb S, Armbyab N (2006). CFD Study of Section Characteristics of Formula Mazda Race Car Wings[J]. Mathematical and Computer Modelling, vol. 43, no.11, pp. 1275-1287
[6] Versteeg, Henk Kaarle; Malalasekera, Weeratunge (2007). an Introduction to Computational Fluid Dynamics: the Finite Volume Method. Pearson Education.
[7] University of Waterloo (2005). Reynolds number and drag on immersed bodies-supplemental lecture.
[8] Yu Kainan, Xie Shibin (2018). Rear Wing Design and Optimization for Formula SAE Car Based on CFD [J]. Journal of Mechanical & Electrical Engineering, vol.35, no.1, pp.3-4.
[9] Ling Jie, & Wang Yi (2019).Numerical Simulation of Circuar Flow Around a Cylinder At Small Reynolds Number. Mechanical Engineering & Automation, vol.213, no.2, pp.87-88.
[10] Wordley S, Saunders J (2006). Aerodynamics for formula SAE: initial design and performance prediction [R]. New York: SAE Technical Paper. Retrieved March 10th 2020.
[11] Zhang Xuan. Analyze and Optimize FSC Racing Outflow Field Based on CFD. (Doctoral dissertation).